Structural Engineering and Mechanics, *Vol. 48, No. 3 (2013) 367-382*
DOI: http://dx.doi.org/10.12989/sem.2013.48.3.367

Study on critical buckling load calculation method of piles considering passive and active earth pressure

Yong-hui Chen[1,2], Long Chen[*1], Kai Xu[3], Lin Liu[1] and Charles W.W. Ng[4]

[1]*Research Institute of Geotechnical Engineering, Hohai University, Nanjing 210098, China*
[2]*Key Laboratory of Ministry of Education for Geomechanics and Embankment Engineering, Hohai University, Nanjing 210098, China*
[3]*Nanjing Hydraulic Research Institute, Nanjing, 210098, China*
[4]*The Hong Kong University of Science and Technology, Hong Kong*

(Received May 8, 2013, Revised September 22, 2013, Accepted October 20, 2013)

Abstract. Different types of long slender pile shall buckle with weak soil and liquefied stratum surrounded. Different from considering single side earth pressure, it was suggested that the lateral earth pressure can be divided into two categories while buckling: the earth pressure that prevent and promotes the lateral movement. Active and passive earth pressure calculation model was proposed supposing earth pressure changed linearly with displacement considering overlying load, shaft resistance, earth pressure at both sides of the pile. Critical buckling load calculation method was proposed based on the principle of minimum potential energy quoting the earth pressure calculation model. The calculation result was contrasted with the field test result of small diameter TC pile (Plastic Tube Cast-in-place pile). The fix form could be fixed-hinged in the actual calculation assuring the accuracy and certain safety factor. The contributions of pile fix form depend on the pile length for the same geological conditions. There exists critical friction value in specific geological conditions that the side friction has larger impact on the critical buckling load while it is less than the value and has less impact with larger value. The buckling load was not simply changed linearly with friction. The buckling load decreases with increased limit active displacement and the load tend to be constant with larger active displacement value; the critical buckling load will be the same for different fix form for the small values.

Keywords: pile; buckling; critical buckling load; active and passive earth pressure considering displacement; fix form

1. Introduction

Long slender piles were widely used in actual engineering, such as TC pile (Chen *et al*. 2008) and Augeo pile (Cortlever and Gutter 2002) used in the embankment engineering or the small diameter micropiles in constructional engineering (Ofner 2007), the slenderness ratio(the ratio of pile length and diameter) reach 70~100 or larger, the critical buckling load analysis become important checking and analyzing contents in engineering designing and theoretical studying under specific geological condition. Experience has shown that, in common situations, surrounding soil

∗Corresponding author, Ph.D. Candidate, E-mail: longchenhhu@163.com

http://www.techno-press.org/?journal=sem&subpage=8 ISSN: 1225-4568 (Print), 1598-6217 (Online)

prevent the pile from buckling. But Granholm (1929) showed that for piles in normal dimensions driven through soft soil, buckling take place in extremely soft soil. Golder and Skipp (1957), Bergfelt (1957) proved that slender piles shall buckle under vertical load and the buckling stress was less than the material yield point stress, it was the same for long piles extend from the ground (Brandtzaeg and Harboe 1957). Accordingly David (2007) proposed that Buckling could control the design of fully embedded piles in some cases (Shield 2007). EN 1997-1 (Chapter 7.8) states that in general it should check buckling of piles which are surrounded by soil with undrained shear strength of c_u<10kPa. The German DIN 1054 (Chapter 8.5.1-2) requires a design check against buckling if piles penetrate soils with c_u < 15kPa. For piles with a diameter smaller than 30cm, DIN 4128 (Chapter 9.8) order a check against buckling while c_u<10kPa. Chinese JGJ 94-2008 adopt stabilizing factor to decreasing the bearing pile capacity. The critical buckling load can be defined as the peak load that holding the pile upright before buckling. It was summed up that the pile under general size shall not be buckling with strong surrounding soil, but different slender piles shall buckle with weak soil surrounded (commonly undrained shear strength c_u<15kPa) and the critical buckling load needed to be checked.

In theory calculations, critical buckling load was calculated based on principle of stationary potential energy (Yang and Song 2000, Zhu 2004, Zhao 1990, Gabr *et al*. 1997), Rayleigh-Ritz method (Reddy and Valsangkar 1970), element-free Galerkin method, finite difference method (Poulos 1969, Poulos and Davis 1980), and numerical simulation method (Davission and Robinson 1965), different influencing factors such as the shaft resistance (Reddy and Valsangkar 1970), earth pressure (Gabr *et al*. 1997), layered foundation soil (Lin and Chang 2010), scour (Lin *et al*. 2010), earthquake (Haldar and Babu 2010, Dasha *et al*. 2010), initial geometric imperfection (Tomas and Tovar 2012) and so on were studied. The earth pressure was though to prevent pile from buckling (simulated by *m* method, *c* method, *k* method) traditionally, but the calculation method used has larger calculation error and cannot take the active effect on pile buckling. The author suggested that the lateral earth pressure can be divided into two categories in the moment of pile buckling: the earth pressure that prevent and promote the lateral movement. Buildings such as dockside pile, pit side pile, deep basement side column that one side was air or water, under vertical load, the lateral earth pressure shall promote the pile or Column to buckling. The disadvantage was outstanding and could not be ignored, first discussed by Vogt *et al.* (2009).

Distinguished from using horizontal resistance coefficient of the soil, the earth pressure calculation model was proposed suppose that the pressure linearly changed with the horizontal displacement, make Rankine earth pressure to be the limit values. Critical buckling load calculation method in three common constraint forms of the pile: hinged-hinged, fixed-hinged, fixed-fixed was proposed based on the principle of minimum potential energy quoting calculation model of active and passive earth pressure considering displacement considering overlying load, shaft resistance, earth pressure at both side of the pile. The calculation result was contrasted with the field test result of small diameter Plastic Tube Cast-in-place pile (TC pile), at the same time, the influence of the constraint form and s_a (the displacement of the soil when the Rankine earth pressure were reached) on the slender pile's critical buckling load was studied.

2. Earth pressure calculation model considering displacement

In current critical buckling load calculation theory, horizontal resistance coefficient m was used to calculate the soil resistance value which was consulted from the relative specifications. It valued

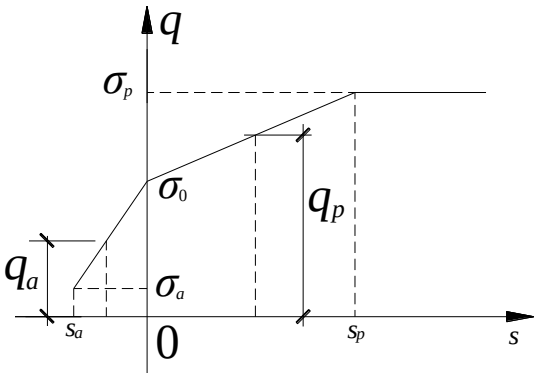

Fig. 1 Earth pressure calculation model considering displacement

fuzzily and there exists differences from the true values in site at the same time the calculate result considering only one side earth pressure. The earth pressure can be divided into two categories in the moment of pile buckling: one was called instantaneous passive earth pressure (noted q_p) that prevent the pile's lateral movement, its limit value was limit passive earth pressure (noted σ_p) at limit passive displacement (noted s_p); the other was called instantaneous active earth pressure (noted q_a) that prevent the pile's lateral movement, its limit value was limit active earth pressure (noted σ_a) at limit active displacement (noted s_a).

According to Mohr's stress circle, earth pressure experience the maximum and minimum principal stress under different displacement, i.e., limit passive and active earth pressure of the surround soil supply for the pile (namely Rankine passive and active earth pressure)

$$\begin{cases} \sigma_p = (\gamma_s z + p_s)K_p + 2c_s\sqrt{K_p} \\ \sigma_a = (\gamma_s z + p_s)K_a - 2c_s\sqrt{K_a} \\ \sigma_0 = (\gamma_s z + p_s)K_0 \end{cases} \tag{1}$$

Where K_p is coefficient of passive earth pressure, $K_p=\tan^2(45^\circ + \varphi/2)$, K_a is coefficient of active earth pressure, $K_a=\tan^2(45^\circ - \varphi/2)$, K_0 is coefficient of earth pressure at rest, p_s is load between the piles (kN/m^2), γ_s is soil gravity (kN/m^3) valued float gravity under water, c_s and φ are cohesion (kPa) and internal friction angle ($^\circ$) of the soil, z is the depth (m).

The influence factors such as overlying load, consolidation of the surrounding soil et al can be completely considered by approximate simulation of the active and passive earth pressure. The c, φ value was determined more empirical and liable than m value in m method.

As shown in Fig. 1, the earth pressure was supposed linearly change with the horizontal displacement according to Fig. 13.7 in the famous textbook Soil Mechanics by Lambe and Whitman (1969). At active condition, q_a was linearly decreased with increasing displacement; σ_a was reached when the displacement was s_a. q_a approached to a definite value for displacement larger than s_a. At passive condition, q_p was linearly increased with increasing displacement, σ_p was reached for displacement was s_p. q_p approached to a definite value for displacement larger than s_p. The instantaneous active and passive earth pressure calculation method were (the displacement value was set to be positive).

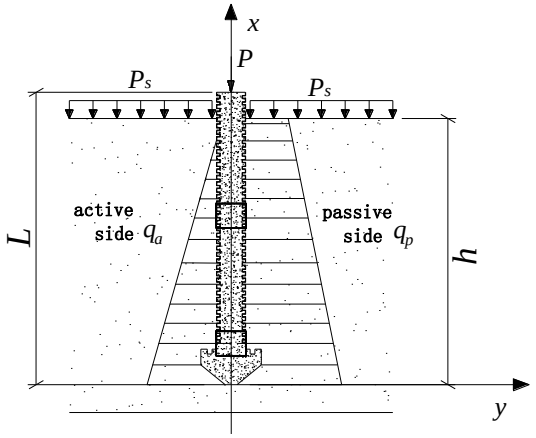

Fig. 2 Coordinate system of critical buckling load calculation

$$q_a=\begin{cases}B(\sigma_0-\dfrac{\sigma_0-\sigma_a}{s_a}s) & s<s_a\\ B\sigma_a & s>s_a\end{cases};\quad q_p=\begin{cases}B(\sigma_0+\dfrac{\sigma_p-\sigma_0}{s_a}s) & s<s_p\\ B\sigma_p & s>s_p\end{cases} \tag{2}$$

Where B is the pile width used in the calculation. For circular pile, B was needed to set to rectangle pile's calculation width equivalently, the conversion formula was $B=K_fK_0Kb$. Where K_f was shape conversion factor i.e., the pile width at the force direction multiplied by makes the equivalent rectangle pile with; K_0 was force conversion factor which was used to simplified the actual space earth pressure bearing lateral load; K was interaction coefficient between piles. The formula was complicated and the factors K_f and K_0 that do not have sufficient theoretical and practical basis were difficult to determine. Above all, Wei (2009), Yao *et al.* (2009), proposed a simplified calculation method, for circular pile, B=0.9(1.5d+0.5) for $d\leq$1m, B=0.9(d+1) for d>1m.

3 Critical buckling load calculation methods

Slenderness piles that inserted in the weak soft soils shall buckle under vertical load, these pile show varying degree of horizontal displacement along the length while buckling. The minimum vertical load while horizontal displacement happens was called critical buckling load. The maximum horizontal displacement of the pile can occur was extremely tiny and the pile shall crush with no sign if the displacement was larger than the maximum value. So the pile can be considered to be broken while horizontal displacement happens and the critical buckling load calculated using energy method corresponding to the moment that the horizontal displacement for happening without happening needless to consider the limit value. Based on the above, the instantaneous active and passive earth pressure can be thought to be linearly changed in the calculation process showed in Chapter 2. Small pile deformation assumption was adopted to the calculation in this paper.

The coordinate system was established shown in Fig. 2, without considering the axis deformation and shearing deformation, the total potential energy of the pile can be expressed as follows

$$\Pi = U - V = \frac{1}{2}\int_0^L EI\left[(d^2y/dx^2)^2/(1+(dy/dx)^2)^3\right]dx + \frac{1}{2}\int_0^h (q_p+\sigma_0)ydx - \frac{1}{2}\int_0^h (q_a+\sigma_0)ydx - \int_0^L P(x)(\sqrt{1+(dy/dx)^2}-1)dx \tag{3}$$

Factoring polynomials neglecting items with power more than 4, the equation can be simplified as

$$\begin{aligned}\Pi &= U - V \\ &= \frac{1}{2}\int_0^L EI(y'')^2[1-3(y')^2]dx + \frac{1}{2}\int_0^h (q_p - q_a)ydx - \frac{1}{2}\int_0^L P(x)[\frac{1}{2}(y')^2 - \frac{1}{8}(y')^4]dx \\ &= \frac{1}{2}\int_0^L EI(y'')^2dx + \frac{1}{2}\int_0^h q_p ydx - \frac{1}{2}\int_0^h q_a ydx - \frac{1}{2}\int_0^L P(x)(y')^2dx\end{aligned} \tag{4}$$

Where U notes the strain energy of the system due to the bending of the pile and elastic deformation of soil, V notes the potential energy of external load, L notes total pile length (m), h denote embedded length of pile (m), EI notes flexural stiffness of pile (kN·m^2), $P(x)$ notes axial force (kN), q_a = the instantaneous active earth pressure, q_p notes the instantaneous passive earth pressure, the calculation depth $z=h-x$, x notes the length of the calculation position to the pile tip.

While shaft resistance and the pile gravity were taken into account, the axial force $P(x)$ of any section underground can be written as

$$P(x) = P_P + A\gamma_C(L-x) - f(h-x) = P_P + (A\gamma_c L - fh) - (A\gamma_c - f)x \tag{5}$$

Where P_P notes the vertical load at the top of pile (kN), f notes pile friction eigenvalue (kN/m), γ_c notes concrete gravity (kN/m^3), A notes the cross-sectional area of the pile (m^2), suppose $\lambda_1 = A\gamma_c L - fh$; $\lambda_2 = A\gamma_c - f$。

The total potential energy of the pile can be expressed simplify as follows

$$\Pi = U + V = \frac{1}{2}\int_0^L EI(y'')^2dx + \frac{1}{2}\int_0^h q_p ydx - \frac{1}{2}\int_0^h q_a ydx - \frac{1}{2}\int_0^L (P_p + \lambda_1 - \lambda_2 x)(y')^2dx \tag{6}$$

It is necessary to integrate q_a in the intervals separately in [0, h] for q_a values with interval. For embankment piles that belong to completely buried pile was studied in this paper in the equation $h=L$. And the following 3 cases were studied:

Case 1 Top hinged tip hinged pile (hinged-hinged pile) calculation model

The deflection curve function about hinged-hinged pile is

$$y = \sum_{n=1}^{\infty} C_n \sin\frac{n\pi x}{l} \tag{7}$$

Supposed half-wave number n equals *1*, the yield modal was

$$y(x) = c\sin\pi\frac{x}{l} \tag{8}$$

Where: c was the amplitude of the yield modal.

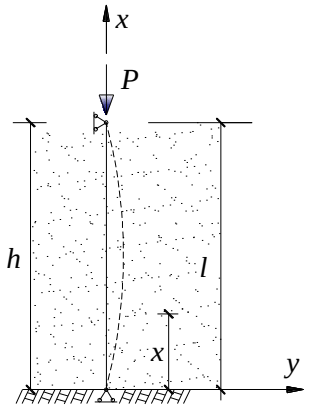

Fig. 3 Calculate model for top hinged, tip hinged pile

Substitute the yield modal equation into Eq. (4)

$$\begin{aligned}\Pi &= U - V \\ &= \frac{1}{2}\int_0^L EI(y'')^2 dx + \frac{1}{2}\int_0^h q_p y dx - \frac{1}{2}\int_0^h q_a y dx - \frac{1}{2}\int_0^L P(x)(y')^2 dx \\ &= \frac{1}{2}\int_0^L EI(y'')^2 dx + \frac{1}{2}\int_0^h B(\sigma_0 + \frac{\sigma_p - \sigma_0}{s_p} y) y dx - \frac{1}{2}\int_0^h B(\sigma_0 - \frac{\sigma_0 - \sigma_a}{s_a} y) y dx - \frac{1}{2}\int_0^L P(x)(y')^2 dx \\ &= \frac{1}{8L^3 s_a s_p} c_s^2 \left(\begin{array}{l} 4L^4 c_s \sqrt{K_p} s_a - 2L^4 K_0 P_s s_a + 2L^4 K_p P_s s_a + 4L^4 c_s \sqrt{K_a} s_p + 2L^4 K_0 P_s s_p - 2L^4 K_a P_s s_p + 2EI\pi^4 s_a s_p \\ -2L^2\pi^2 p_p s_a s_p - L^5 K_0 s_a \gamma_s + L^5 K_p s_a \gamma_s + L^5 K_0 s_p \gamma_s - L^5 K_a s_p \gamma_s - 2L^2\pi^2 s_a s_p \lambda_1 + L^3\pi^2 s_a s_p \lambda_2) \end{array} \right)\end{aligned} \tag{9}$$

According to the principle of stationary potential energy, it obtained

$$p_p = \frac{1}{2L^2\pi^2 s_a s_p} \left[\begin{array}{l} 4L^4 c_s (\sqrt{K_p} s_a + \sqrt{K_a} s_p) + 2L^4 (K_p - K_0) P_s s_a \\ +2L^4 (K_0 - K_a) P_s s_p + 2EI\pi^4 s_a s_p + L^5 (K_p - K_0) s_a \gamma_s \\ +L^5 (K_p - K_a) s_p \gamma_s - 2L^2\pi^2 s_a s_p \lambda_1 + L^3\pi^2 s_a s_p \lambda_2) \end{array} \right] \tag{10}$$

There were many unknown numbers in the equation and have complex form. If k_a=0,k_p=0,k_0=0,λ_1=0, λ_2=0, we will get

$$p_p = \frac{EI\pi^2}{L^2} \tag{11}$$

It was the expression of Euler critical load value for hinged-hinged rod.

Case 2 Top fixed tip hinged pile (fixed-hinged pile) calculation model

The boundary conditions of the deflection curve for fixed - hinged pile were:
x=0, y=0 and *x=l, y=0, y'=0*

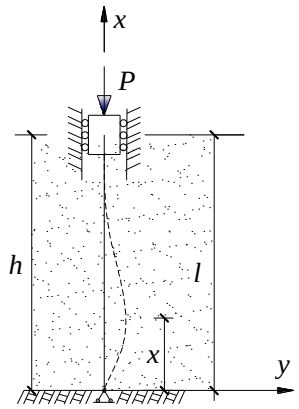

Fig. 4 Calculate model for fixed-hinged pile

And the deflection curve was

$$y=\sum_{n=1}^{\infty}C_n f_n(x)=\sum_{n=1}^{\infty}C_n[\cos(\frac{(2n+1)\pi}{2}\frac{l-x}{l})-\cos(\frac{(2n-1)\pi}{2}\frac{l-x}{l})] \tag{12}$$

Suppose half-wave number n equals *1*, the yield modal was

$$\begin{aligned} y(x)&=c[\cos(\frac{3\pi}{2}-\frac{3\pi}{2}\frac{x}{l})-\cos(\frac{\pi}{2}-\frac{\pi}{2}\frac{x}{l})] \\ &=-c\sin(\frac{\pi x}{2L})-c\sin(\frac{3\pi x}{2L}) \end{aligned} \tag{13}$$

Where: c was the amplitude of the yield modal.

Substitute the yield modal equation into energy c

$$\begin{aligned} \Pi&=U-V \\ &=\frac{1}{2}\int_0^L EI(y'')^2[1-3(y')^2]dx+\int_0^h q_p y dx-\int_0^h q_a y dx-\int_0^L P(x)[\frac{1}{2}(y')^2-\frac{1}{8}(y')^4]dx \\ &=\frac{1}{2}\int_0^L EI(y'')^2[1-3(y')^2]dx+\int_0^h B(\sigma_0+\frac{\sigma_p-\sigma_0}{s_p}y)ydx-\int_0^h B(\sigma_0-\frac{\sigma_0-\sigma_a}{s_a}y)ydx \\ &\quad-\int_0^L P(x)[\frac{1}{2}(y')^2-\frac{1}{8}(y')^4]dx \\ &=\frac{41c_s^2EI\pi^4}{32L^3}+\frac{c_s^2L\left\{18\pi^2[2c_t\sqrt{K_a}+(K_0-K_a)P_s]+L(16+9\pi^2)(K_0-K_a)\gamma_s\right\}}{36\pi^2 s_a} \\ &\quad+\frac{c_s^2L\left\{18\pi^2[2c_s\sqrt{K_p}+(K_p-K_0)P_s]+L(16+9\pi^2)(K_p-K_0)\gamma_s\right\}}{36\pi^2 s_p} \\ &\quad-\frac{c_s^2[10\pi^2(p_p+\lambda_1)+L(16-5\pi^2)\lambda_2]}{16L} \end{aligned} \tag{14}$$

Software Mathematica was used to calculate according to the principle of stationary potential energy for the equation was complex. And the unknown number was

$$p_p = \frac{1}{180L^2\pi^4 s_a s_p}\begin{bmatrix} 288L^4\pi^2 c_s(\sqrt{K_p}s_a - \sqrt{K_a}s_p) + 144L^4\pi^2(K_p - K_0)P_s s_a + 144L^4\pi^2(K_0 - K_a)P_s s_p \\ +369EI\pi^6 s_a s_p + 128L^5(K_p - K_0)s_a\gamma_s + 72L^5\pi^2(K_p - K_0)s_a\gamma_s + 128L^5(K_0 - K_a)s_p\gamma_s \\ +72L^5\pi^2(K_0 - K_a)s_p\gamma_s - 180L^2\pi^4 s_a s_p\lambda_1 - 288L^3\pi^2 s_a s_p\lambda_2 + 90L^3\pi^4 s_a s_p\lambda_2 \end{bmatrix} \quad (15)$$

If ignoring the pile gravity, earth pressure of the surrounding soil, overlying load and so on, the result can be expressed as

$$p_p = \frac{369EI\pi^2}{180L^2} \approx \frac{EI\pi^2}{0.49l^2} = \frac{EI\pi^2}{(0.7l)^2} \quad (16)$$

The result equals the Euler critical load expression, Euler rod can be a special case of the calculation model.

Case 3 Top fixed tip fixed pile (fixed-fixed pile) calculation model

The deflection curve boundary conditions were:

x=0,y=0， *y'=0*; *x=l*, *y=0*， *y'=0*

So the deflection curve can be expressed as

$$y = \sum_{n=1}^{\infty} C_n f_n(x) = \sum_{n=1}^{\infty} C_n[1 - \cos(\frac{2n\pi x}{L})] \quad (17)$$

Suppose half-wave number *n* equals *1*, the yield modal was

$$y(x) = c[1 - \cos(\frac{2\pi x}{L})] \quad (18)$$

Where: *c* was the amplitude of the yield modal.

Substitute the yield modal equation into energy Eq. (6)

$$\begin{aligned} \Pi &= U - V \\ &= \frac{4c_s^2 EI\pi^4}{L^3} + \frac{3c_s^2 L[4c_t\sqrt{K_p} + (K_p - K_0)(2P_s + L\gamma_s)]}{8s_p} \\ &\quad + \frac{3c_s^2 L[4c_s\sqrt{K_a} + (K_0 - K_a)(2P_s + L\gamma_s)]}{8s_a} - \frac{c_s^2\pi^2(2p_p + 2\lambda_1 - L\lambda_2)}{2L} \end{aligned} \quad (19)$$

According to the principle of stationary potential energy

$$p_p = \frac{1}{8L^2\pi^2 s_a s_p}\begin{bmatrix} 32EI\pi^4 s_a s_p + 12c_s L^4(\sqrt{K_p}s_a + \sqrt{K_a}s_p) + 6L^4(K_p - K_0)P_s s_a \\ +6L^4(K_0 - K_a)P_s s_p + 3L^5(K_p - K_0)s_a\gamma_s + 3L^5(K_0 - K_a)s_p\gamma_s \\ -8L^2\pi^2 s_a s_p\lambda_1 + 4L^3\pi^2 s_a s_p\lambda_2 \end{bmatrix} \quad (20)$$

If ignoring the pile gravity, earth pressure of the surrounding soil, overlying load and so on, the result can be expressed as

$$p_p = \frac{4EI\pi^2}{L^2} = \frac{EI\pi^2}{(0.5l)^2} \tag{21}$$

The result equals the Euler critical load expression, Euler rod can be a special case of the calculation model.

4. Case verification

4.1 Geological conditions

A practical engineering project with weak soft soil disposed with TC pile (Plastic Tube Cast-in-place Concrete pile). TC pile was made up of precast reinforced concrete pile tip, single-walled threaded PVC plastic tube, concrete pile cap, concrete in the tube and reinforcing steel bar in the pile. The plastic tube was firstly driven into the ground by machines consists of excavator, frame, sinking tube and vibrating hammer and so on. Then different from other precast pile, according to the TC pile construction technology, water was poured into the plastic tube to balance the surrounding earth pressure avoiding broken while driving each tube into the ground, then concrete pile and pile cap were poured integrate after pump water out from the driven tubes in site together to ensure the quality. The TC pile diameter was 160mm, the driven depth was 10~20m, and the slenderness ratio reach 62.5-125.

Physical and mechanical properties of every layer soil were showed in Table 1. Through drilling exploration, The 1st layer soil was asymmetrically distributed with clay partly with silty clay, mainly was soft plastic. The 2nd layer soil was the same but with high toughness. The 3rd layer soil was weak soft soil, silt, soft plastic with high compression. The 4th layer was silty clay contain breccia with medium compression. The 5th layer soil was medium weathered condensate sandstone with high ground bearing capacity that can provide steady support. Vane shear test was carried out and the result was showed in the Fig. 5. The undrained shear strength of most of the surrounding soil was less than 15kPa that belong to weak soft soil.

While the pile was driven into the supporting stratum in construction process, the pile driver exerted centrifuge force to the immersed tube to carry out vibration pile driving. It made the pile tip supported steady by the supporting stratum but cannot be inserted it deeper because of the limit weight of the pile driver. So the pile tip fixed form usually between hinged and fixed. The pile top can thought to be fixed because of the pile and pile cap (20cm thick) were poured together and reinforcing steel bar in the pile and the pile cap were joint. Bearing capacity test was carried out on 4 TC piles in site and low strain dynamic testing was used to identify the broken place.

Table1 The physical-mechanical properties of soil layers

N	Soil type	*H*/m	γ/kN/m^3	*c*/kPa	ϕ/°	f_{ak}/kPa
1	Clay	0.60	18.7	21	6.8	70
2	Clay	0.60	17.5	22.4	5.1	60
3	Silt	10.00	16.3	8.3	0.7	45
4	Silty clay	2.30	19.1	--	--	250
5	Sandstone	--	--	--	--	1000

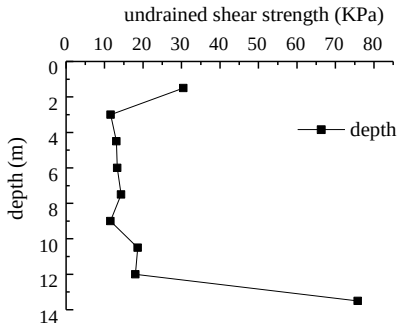

Fig. 5 Undrained shear strength varied with depth

4.2 In site single pile test result

As shown in Fig. 5 the undrained shear strength of most of the surrounding soil was less than 15kPa that cannot supply effective lateral support. The length of TC pile was designed according to the depth of the medium weathered condensate sandstone, so the TC pile was end bearing pile.

Because of the particularity of the site geological conditions, the test piles were broken and the crack can be heard on the ground while the ultimate load was reached. The test results were showed in Table 2 and Fig. 6, NO. 1 pile with 14.51m length cracked at 175kN and the broken section located at a depth of 8.8m according to small strain test, NO. 2 pile with 14.06m length cracked at a depth of 5.28m under 175kN load, NO.3 pile with 13.2m length cracked at a depth of 4.04m under 168kN, NO.4 with 13.1m length cracked at a depth of 7.03m under 189kN. The ultimate bearing capacity was 239kN determined by the strength of pile ultimate bearing capacity, the measured results account 70%~79%, so it can be sure that the crack was not produced by compression failure of pile.

In the engineering geological conditions, TC pile was long slender pile and the surrounding soil cannot supply effective lateral support, the pile was easy to buckle with lateral displacement. The pile's cross-section force turned small eccentricity into large eccentricity while lateral horizontal displacement occurred under vertical load; tensile stress appeared in the cross-section edge, effective compression area is reduced and the maximum compression stress increased. Tensile failure happens while the tensile stress was larger than the concrete tensile strength, compression failure happens while the compression stress was larger than the concrete compression strength. Stress was redistributed for reduced effective compression area while any failure form of the two happens, leading to farther crack in the cross-section gradually. So macro pile destroys instantaneously under vertical load just like the crake in the test and the ultimate load was less than the load determined by the pile material. Both tensile damage and compression damage were caused by the lateral horizontal displacement of the pile during buckling, so the two damages can be attributed to buckling failure. But it should be noted that the ultimate load got from the field test was not the critical buckling load which corresponding to the instability not destruction of the pile. So the pile was buckling first and then broken for small displacement. The ultimate load was approximately equal to the critical buckling load and it was easier to get the ultimate load in field test, so the load get from the test can be used in some degree. Above all, the author though piles buckling in the field test and the ultimate load can be compared to the critical buckling load calculated method built above.

Table 2 Summary of the single pile load test result

Pile number	Length/m	Ultimate load capacity/kN	Broken location/m
1	14.51	175	8.8
2	14.06	175	5.28
3	13.2	168	4.04
4	13.1	189	7.03

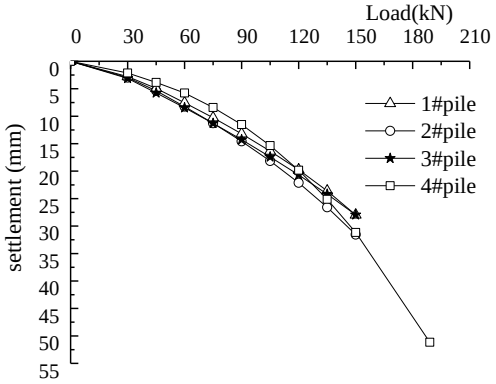

Fig. 6 The result of the single pile load test

The pile length equals the inserted depth of the pile according to the TC pile construction technology. Suppose the design class of concrete was C25, the axial tensile design strength f_c=11.9MPa, young's modulus E=2.8×10^{9}kPa, concrete bulk density γ_c=23kN/m^3, pile diameter d=(0.145+0.16)/2=0.1525m for threaded tube, calculate width B=0.9×(1.5×0.1525+0.5)=0.66m. The surrounding soil was simplified into one uniform soil stratum, average weighted cohesion c_s=9.74kPa, internal friction angle φ=1.26°, floating bulk density γ_s=16.94kN/m^3, skin friction f=10kPa.

S_a for cohesive soil was 0.001H~0.005H referring to active and passive earth pressure test results of retaining walls. The pile length usually was 9~15m, s_a and s_p value can be defined 10mm and 150mm (Mei and Zai 2001). The maximum horizontal displacement of the concrete pile was less than s_a, so the instantaneous active and passive earth pressure can be expressed linearly with the displacement. Compared the calculate results with test results based on the critical buckling load calculation model with top hinged tip hinged, top fixed tip hinged, top fixed tip hinged built above, and the influence of fixed form on critical buckling load was studied.

Fig. 7(a) shows the calculation result and the test result for 3 ideal fix forms, the test results are intermediate between the calculate results of fixed-hinged pile and fixed-fixed pile. Let the test result to be unit 1, Fig. 7(b) shows the ratio of calculated result and test result for 4 test piles. Calculated result for top fixed tip hinged, top fixed tip fixed takes 0.843~0.946 and 1.198~1.361 of the test result respectively. The pile tip fix form was between hinged and fixed by the above analysis and the fix form can be thought to be hinged in the site through the calculation achievement ensuring accuracy with safety factor.

Table 3 Comparison of calculated and tested results

Pile type	Pile length/m	Critical buckling load/kN			Ultimate load	Ratio of the loads		
		According to case 1/kN	According to case 2/kN	According to case 3/kN	kN	ξ_1	ξ_2	ξ_3
TC pile	14.51	117.92	155.648	209.618	175	0.674	0.889	1.198
TC pile	14.06	115.836	156.196	215.175	175	0.662	0.893	1.230
TC pile	13.2	112.87	158.902	228.71	168	0.672	0.946	1.361
TC pile	13.1	112.62	159.375	230.565	189	0.596	0.843	1.220

*Note: ξ_1 was the ratio of calculation result according to case 1 (hinged - hinged) and test result, ξ_2 was the ratio of calculation result according to case 2 (fixed - hinged) and test result, ξ_3 was the ratio of calculation result according to case 3 (fixed - fixed) and test result.

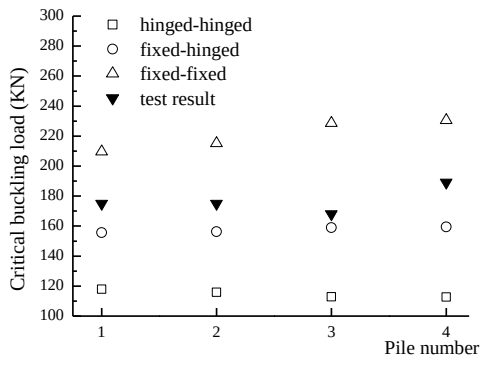

(a) Figure of calculate result versus filed test result

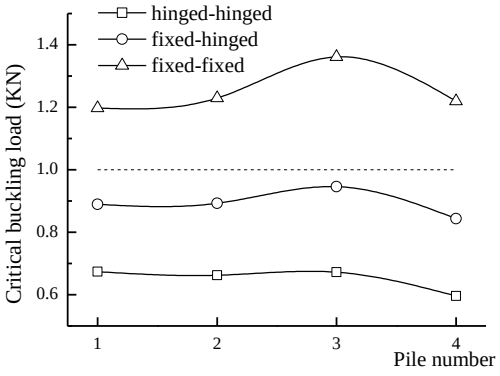

(b) Figure of ratio of calculate result versus filed test result

Fig. 7 Critical buckling load of different fix form piles

5. Parametric analysis

5.1 The influence of the fixation

Fig. 8 show different ratios of fixed-hinged and fixed-fixed to hinged-hinged separately, the two horizontal dotted lines was that ratio calculated from Euler rod. In the geological conditions, the critical buckling load increase 30%~40% or more while the pile fix form turn from hinged–hinged to fixed-hinged, 77%~104% for pile fix form turn hinged-hinged to fixed-fixed. There are some differences between the results from Euler theory and the calculation model in this paper, they will be the same with decreased pile length. Large critical buckling load improved value of the two relative fix forms with the decrease pile length. The contributions of pile fix form depend on the pile length for the same geological conditions.

5.2 The influence of the side friction

Through computation and analysis for 13.1m pile length based on the field test data, the influence of side friction was studied.

Fig. 9(a) is figure of critical buckling load change with side friction. It show that side friction was one of important infulence on the critical buckling load, critical buckling load of 3 fixed forms inreases linearly with increased side friction value, the critical buckling load increases from 81.26kN to 191.03kN, 117.84kN to 263.21kN, 199.2kN to 308.98kN with side friction inreases from 0 to 35kPa for hinged-hinged, fixed-hinged, fixed-fixed pile respectively. Critical buckling load increase ratio defined as the ratio of critical buckling load value after increased side friction and that before the increased. As show in Fig. 9(b) side friction has slightly less impact on fixed-fixed pile than hinged-fixed pile and hinged-hinged pile. The ratio decreased from 7% to 1% gradually with the side friction increased from 0 to 30 kPa for the latter two fix forms. The ratio was dropped while the side friction was 30kPa, in means that side friction has little effect on the critical buckling load exceeding 30kPa in the geological conditions. So there exist one friction value in specific geological conditions that the side friction has larger impact on the critical buckling load while it is less than the value and less impact with larger value, not the simply linearly relationship showed by Fig. 9(a).

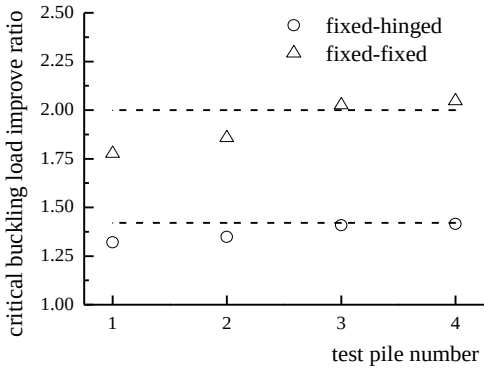

Fig. 8 Critical buckling load improvement caused by the fixation mode

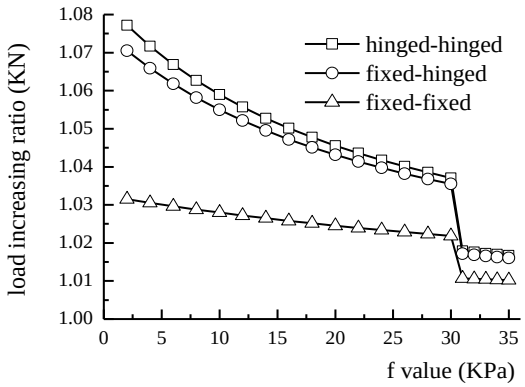

(a) Figure of critical buckling load and side friction

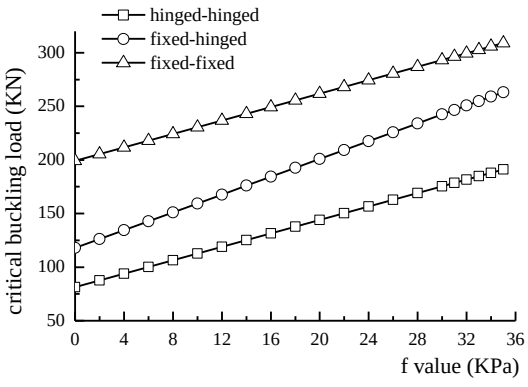

(b) Figure of critical buckling load increase ratio and side friction

Fig. 9 Influence of side friction on critical buckling load

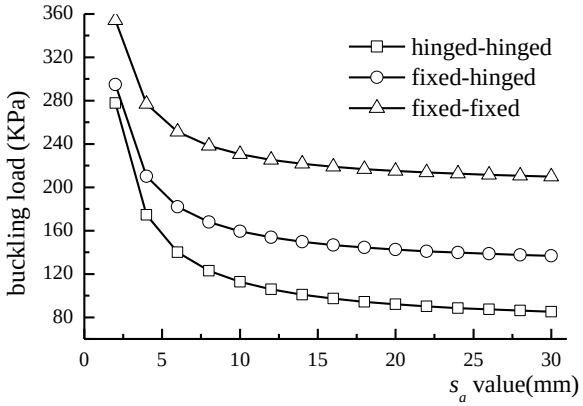

Fig. 10 critical buckling load - s_a

5.3 Influence of s_a and s_p

Lateral earth pressure considering displacement was adopted in the critical buckling load calculation model for the first time in this paper. The influence of s_a and s_p on limit active and passive earth pressure was studied based on the assumption that s_p=15s_a which refers to past research experience.

Fig. 10 shows the critical buckling load change with s_a value, the buckling load decreases with increase s_a and the load tend to be constant with larger s_a value. If the s_a value is small enough the critical buckling load will be the same for different fix form. At the same s_a value the critical buckling load for fixed-fixed pile> fixed-hinged pile > hinged-hinged pile.

6. Conclusions

Different types of slenderness pile shall buckle with weak soil and liquefied stratum surrounded. The critical buckling load calculation method was proposed in this paper and the main conclusions were:

• Critical buckling load calculation method in three common constraint forms of the pile: hinged-hinged, fixed-hinged, fixed-fixed were proposed based on the principle of minimum potential energy quoting calculation method of active and passive earth pressure considering displacement considering overlying load, shaft resistance, earth pressure at both side of the pile.

• For TC pile projects, the calculated critical buckling load was compared with the test results. The test result value was on the regions between the critical buckling load calculated for fixed-hinged pile and fixed-fixed pile. The calculate results were 0.843-0.946 and 1.198-1.361. The fix form can be fixed-hinged in the actual calculation assuring the accuracy and certain safety factor.

• The influence of fixation, side friction and limit active and passive displacement were discussed through parametric study. The influence of fixed form on the critical buckling load depends on the pile length.

• The calculation of critical buckling load was restricted by multiplex factors and complexity. The earth pressure calculation model suggested in this paper needs to be further examined through

experimental and engineering practice and both limit active and passive displacement value needs to be further studied.

Acknowledgement

This study was supported by the National Natural Science Foundation of China under Grant No.51178160 and Jiangsu Province Graduate Education Innovation Program under Grant NO.CXZZ11-0431. Grateful appreciation is expressed for the supports.

References

Chen, Y.H., Cao, D.H., Wang, X.Q., Du, H.W. and Zhang, T. (2008), "Field study of plastic tube cast-in-place concrete pile", *Journal of Central South University of Technology*, **15**(S2), 195-202.

Cortlever, N.G. and Gutter, H.H. (2002), "Design of double track railway Bidor-Rawang on AuGeo piling system according to BS8006 and PLAXIS numerical analysis", http://cofra.sk/files/documents/technicke_spravy/kl2002augeo.pdf.

Golder, H.G. and Skipp, B.O. (1957), "The buckling of piles in soft clay", *Proceedings of the 4th Int. Conf. on Soil Mech. and Found. Eng.*, London, England.

Bergfelt, A. (1957), "The axial and lateral load bearing capacity, and failure by buckling of piles in soft clay", *Proceedings of the 4th Int. Conf. on Soil Mech. and Found. Eng.*, London, England.

Brandtzaeg, A. and Harboe, E. (1957), "Buckling tests of slender steel piles in soft, quick clay", *Proceedings of the 4th. Int. Conf. Soil Mech. Found. Eng*., 19-23.

Dasha Suresh, R., Subhamoy, B. and Anthony. B. (2010), "Bending–buckling interaction as a failure mechanism of piles in liquefiable soils", *Soil Dynamics and Earthquake Engineering*, **30**(1-2), 32-39.

Davisson, M.T. and Robinson, K.E. (1965), "Bending and buckling of partially embedded piles", *Proceeding 6th International Conference on Soil Mechanics and Foundation Engineering*, Toronto, University of Toronto Press.

Gabr, M.A., Wang, J.J. and Zhao, M. (1997), "Buckling of piles with general power distribution of lateral subgrade reaction", *Journal of Geotechnical and Geoenvironmental Engineering*, **123**(2), 123-130.

Haldar, S. and Babu, G.L.S. (2010), "Failure mechanisms of pile foundations in liquefiable soil: parametric study", *International Journal of Geomechanics*, **10**(2), 74-83.

Lambe, T.W. and Whitman, R. (1969), *Soil mechanics*, Massachusetts Institute of Technology, John Wiley & Sons, New York.

Lin, S.S. and Chang, W.K. (2010), "Buckling of piles in a layered elastic medium", *Journal of the Chinese Institute of Engineers*, **25**(2), 157-169.

Lin, C., Bennett, C., Han, J. and Parsons, R.L. (2010), "p-y based approach for buckling analysis of axially loaded piles under scoured conditions", *Structures Congress*, 110-120.

Mei, G.X. and Zai, J.M. (2001), "Rankine earth pressure model considering deformation", *Chinese Journal of Rock Mechanics and Engineering*, **20**(6), 851-854.

Ofner, R. and Wimmer, H. (2007), "Buckling resistance of micropiles in varying soil layers", *Bautechnik*, **84**(12), 881-890.

Poulos, H.G. and Davis, E.H. (1980), *Pile Foundation Analysis and Design*, The University of Sydney, Sydney.

Poulos, H.G. and Mattes, N.S. (1969), "The behaviour of axially loaded end-bearing pile", *Geotechnique*, **19**(2), 285-300.

Reddy, A.S. and Valsangkar, A.J. (1970), "Buckling of fully and partially embedded piles", *Journal of Soil Mechanics and Foundation*, **96**(6), 1951-1965.

Shields, D.R. (2007), "Buckling of micropiles", *Journal of Geotechnical and Geoenvironmental Engineering*, **133**(3), 334-337.
Tomas, A. and Pedro, T.J. (2012), "The influence of initial geometric imperfections on the buckling load of single and double curvature concrete shells", *Computers and Structures*, **96-97**, 34-45.
Vogt, N., Vogt, S. and Kellner, C. (2009), "Buckling of slender piles in soft soils", *Supplement: Geotechnical Engineering*, **86**(S1), 98-112.
Wei, D.X. (2009), "Research on the calculation method for elastic long pile under horizontal load", Southwest Jiaotong University, Chengdu.
Yang, W.H. and Song, L. (2000), "Axial buckling analysis for top-free and bottom-fixed pile", *Engineering Mechanics*, **5**, 63-66.
Yao, W.J., Qiu, Y.Z. and Cheng, Z.K. (2009), "Initial post-buckling analysis for super-long rock-socketed piles", *Chinese Journal of Geotechnical Engineering*, **31**(5), 738-742.
Zhu, D.T. (2004), "Stability of friction-bearing piles", *Chinese Journal of Rock Mechanics and Engineering*, **12**, 2106-2109.
Zhao, M.H. (1990), "Buckling analysis and tests of bridge piles", *China Journal of Highway and Transport*, **3**(4), 47-56.

Notations

s_a limit active displacement
σ_a limit active pressure
q_a instantaneous active earth pressure
s_p limit passive displacement
σ_p limit passive pressure
q_p instantaneous passive earth pressure
σ_0 earth pressure at rest
K_p coefficient of passive earth pressure
K_a coefficient of active earth pressure
K_0 coefficient of earth pressure at rest